

The growth of stellar mass black hole binaries trapped in an accretion disk of active galactic nuclei

SHU-XU YI,<sup>1</sup> K.S. CHENG,<sup>1</sup> AND RONALD E. TAAM<sup>2,3</sup>

<sup>1</sup>*Department of Physics, The University of Hong Kong*

<sup>2</sup>*Academia Sinica Institute of Astronomy and Astrophysics, Taipei 10617, Taiwan*

<sup>3</sup>*Department of Physics & Astronomy, Northwestern University, 2145 Sheridan Road, Evanston, IL 60208, USA*

## ABSTRACT

Among the four black hole binary merger events detected by LIGO, six progenitor black holes have masses greater than  $20 M_{\odot}$ . The existence of such massive BHs calls for extreme metal-poor stars as the progenitors. An alternative possibility that a pair of stellar mass black holes each with mass  $\sim 7 M_{\odot}$  increases to  $> 20 M_{\odot}$  via accretion from a disk surrounding a super massive black hole in an active galactic nucleus is considered. The growth of mass of the binary and the transfer of orbital angular momentum to the disk accelerates the merger. Based on the recent numerical work of [Tang et al. \(2017\)](#), it is found that, in the disk of a low mass AGN with mass  $\sim 10^6 M_{\odot}$  and Eddington ratio  $> 0.01$ , the mass of an individual BH in the binary can grow to  $> 20 M_{\odot}$  before coalescence provided that accretion takes place at a rate more than 10 times the Eddington value. The mechanism predicts a new class of gravitational wave sources involving the merger of two extreme Kerr black holes associated with active galactic nuclei and a possible electromagnetic wave counterpart.

*Keywords:* gravitational waves, black holes, AGN

## 1. INTRODUCTION

Since the first detection of gravitational waves (GW) by the Laser Interferometer Gravitational-Wave Observatory (LIGO) in 2015, there have been four confirmed binary black hole merger events ([Abbott et al. 2016a,b, 2017a,b](#)). Six out of the total eight progenitor black holes have mass  $\gtrsim 20 M_{\odot}$ , which may point to new formation mechanisms other than the traditional stellar evolutionary channels. Specifically, [Fryer & Kalogera \(2001\)](#) theoretically estimated the mass distribution of BHs as the evolutionary remnant of massive stars (except for population III stars). The mass of BHs formed in this way can not be in excess of  $\sim 10 - 15 M_{\odot}$ , due to significant wind mass loss. Observations of BHs in X-ray binaries in the Galaxy are in accordance with a similar mass distribution ([Farr et al. 2011](#)).

Low metallicity ( $Z < 0.1 Z_{\odot}$ ;  $Z_{\odot}$  is the solar metallicity) star progenitors can remain more massive throughout their evolution as they undergo less wind mass loss and, therefore, are likely to produce BHs of higher mass. It is generally believed that these low metallicity stars are formed in the early universe ([Dominik et al. 2015](#); [Belczynski et al. 2016](#)), which **seems** in contradiction with the low redshift of the detected GW events (three with  $z \sim 0.1$  and one with  $z \sim 0.2$ ). However, by taking into consideration two factors: 1. a long delay time from the birth of the BH binary to coalescence of  $t_{\text{merge}} \sim 10$  Gyr ([Kinugawa et al. 2014](#)); 2. a significantly higher low-metallicity star formation rate at low redshifts than previously thought ([Hirschauer et al. 2016](#)), this apparent conundrum is solved ([Belczynski et al. 2016](#)).

Here, we propose an alternative evolutionary channel in which BHs with masses greater than  $20 M_{\odot}$  can form without the requirement of a low metallicity environment. Specifically, a pair of stellar mass BHs are trapped by and accreted mass from an ambient accretion disk surrounding a supermassive black hole (SMBH) in an active galactic nucleus (AGN). There are a number of recent theoretical works studying related scenarios. In particular, models involving the formation, migration, trapping, hardening and driven merger of stellar mass BH binaries in an accretion disk of a SMBH have previously been studied most recently by [McKernan et al. \(2012\)](#); [Stone et al. \(2017\)](#); [Bartos et al.](#)

yishuxu@hku.hk

hrspksc@hku.hk

taam@asiaa.sinica.edu.tw

(2017); Leigh et al. (2018). However, based on a simple description of the binary interaction with the disk, it was found that little mass was accreted onto the BHs during their inspiral and migration. Here, we consider the same process, but based on the results of the most recent numerical study of the binary interaction with the circumbinary disk by Tang et al. (2017). It is found that there are possible circumstances under which BHs can accrete a non-negligible amount of material from the disk. In this case, there is no requirement for a low metallicity of the stellar population for the formation of high mass stellar BHs ( $> 20 M_{\odot}$ ).

In this Letter, we describe the evolution of binary BHs in terms of a model of mass accretion and orbital shrinkage of a system embedded in a circumbinary accretion disk in §2. With assumed distributions of initial parameters of the binaries, the distribution of BH mass at coalescence is determined in §3 and the migration of the binary is discussed in §4. Finally, we summarize and discuss the implications of our results in the last section.

## 2. ACCRETION ONTO THE BINARY

For simplicity, we limit our discussion to the case of an equal mass binary ( $M_1 = M_2 = m_{\text{BH}} M_{\odot}$ ). This simplification can be justified by the results of Farris et al. (2014), who find that the mass ratio of a binary embedded within a disk tends to unity in a Keplerian circular orbit. Taking the time derivative of the expression of the orbital angular momentum  $J$ , and with the further assumption that each BH in the binary is accreting at the same rate, we obtain the following relation:

$$\frac{\dot{J}}{J} = \frac{3\dot{M}_{\text{bin}}}{2M_{\text{bin}}} + \frac{\dot{a}_J}{2a}, \quad (1)$$

where  $M_{\text{bin}} = 2m_{\text{BH}} M_{\odot}$  and  $m_{\text{BH}}$  is the dimensionless mass of an individual BH,  $a$  is the orbital separation of the binary,  $\dot{a}_J$  is the time rate of change of  $a$  due to the exchange of angular momentum. The numerical simulations of Tang et al. (2017), which also take account of the dominant torques exerted on the binary system associated with the distortion of the mini disks surrounding the two BHs, can be described by the following empirical relation (with physical unit restored):

$$\dot{J} = (-0.21 \tau_{\text{sink}} + 0.437) \dot{M}_{\text{bin}} \sqrt{GMa}, \quad (2)$$

where  $\tau_{\text{sink}}$  is the dimensionless sink time-scale that describes the mass removal rate (due to accretion onto the BHs). We treat the net accretion rate onto individual BHs  $\dot{m}_{\text{BH}}$  and  $\tau_{\text{sink}}$  as independent parameters. This follows from the fact that  $\tau_{\text{sink}}$  alone does not determine the mass flow rate from the mini disk to the BH without providing the surface density of the mini disk. In addition, the net accretion rate can differ from the mass flow rate in the mini disk as result of, for example, outflows.

Combining equations (1) and (2), we have:

$$\frac{\dot{a}_J}{\dot{m}_{\text{BH}}} = -\gamma \frac{a}{m_{\text{BH}}}, \quad (3)$$

where  $\gamma = 1.68 \tau_{\text{sink}} - 0.496$ . Tang et al. (2017) mentioned that in any physical case  $\tau_{\text{sink}}$  should be larger than 2.1, and  $\tau_{\text{sink}}=5$  corresponds to a slow sink.

The orbital shrinkage rate due to gravitational radiation is given by

$$\dot{a}_{12,\text{GW}} = -7.88 \times 10^{-14} a_{12}^{-3} m_{\text{BH}}^3, \quad (4)$$

where  $\dot{a}_{12,\text{GW}}$  is the  $\dot{a}$  due to GW radiation in unit of  $10^{12}$  cm/yr.

For accretion onto the BH, we assume that its rate is proportional to its mass,

$$\dot{m}_{\text{BH}} = \eta m_{\text{BH}} / \tau_{\text{acc}}, \quad (5)$$

where  $\tau_{\text{acc}}$  is the Eddington accretion time scale equal to  $10^8$  yr (assuming a radiative efficiency of  $\sim 20\%^1$ ), and  $\eta$  is the Eddington ratio.

The total change in the rate of the separation is given by  $\dot{a} = \dot{a}_{\text{GW}} + \dot{a}_J$ , where it is assumed that the individual torque contributions can be linearly added. Although this is a common assumption, nonlinearities may result from distortions of the disk. Combining equations (3, 5 and 6), and eliminating  $t$ , we obtain a differential equation between  $a$  and  $m_{\text{BH}}$ :

$$\frac{da_{12}}{dm_{\text{BH}}} = -\gamma \frac{a}{m_{\text{BH}}} - 7.88 \times 10^{-6} a_{12}^{-3} m_{\text{BH}}^2 \eta^{-1}. \quad (6)$$

<sup>1</sup> A different choice of the radiative efficiency is equivalent to a varies in  $\eta$

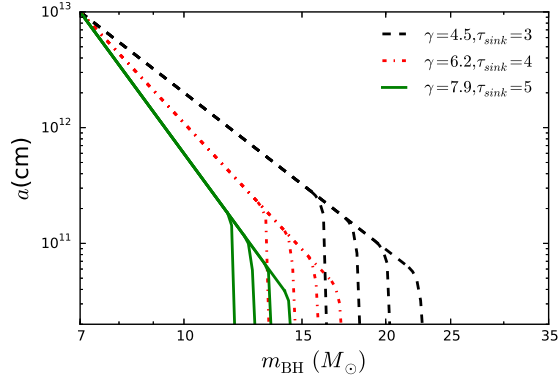


**Figure 1.** The shrinkage of the binary orbital separation as a function of the BH mass. Curves delineated with different line styles and colors correspond to  $\tau_{\text{sink}}$  from 3 to 5 ( $\gamma=4.5$  to 7.9). For each value of  $\gamma$ , four branches are shown corresponding to  $\eta = 1, 10, 100, 1000$  from left to right.

The solution of equation (6) is illustrated in Figure 1 for  $\eta$  ranging from 1 to 1000 and  $\tau_{\text{sink}}$  ranging from 3 to 5. Initially, for large  $a$  and small  $M_{\text{BH}}$ , the shrinkage of  $a$  is dominated by the angular momentum transfer between the binary and the circumbinary disk. Therefore, the dependence of  $a$  on  $M_{\text{BH}}$  is given by a power law,

$$a = a_0 \left( \frac{m_{\text{BH}}}{m_{\text{BH},0}} \right)^{-\gamma}, \quad (7)$$

where  $a_0$  and  $m_{\text{BH},0}$  is the initial separation and the BH mass (dimensionless) respectively. When  $a$  is sufficiently small, GW radiation dominates the evolution, resulting in the turn over in Fig. 1.

The final mass of the BH before coalescence can be evaluated approximately by equating the  $\dot{a}_J$  and  $\dot{a}_{\text{GW}}$  :

$$\gamma \frac{a_{12}}{m_{\text{BH}}} = 7.88 \times 10^{-6} a_{12}^{-3} m_{\text{BH}}^2 \eta^{-1}. \quad (8)$$

Eliminating  $a$  with equation (7), we have:

$$m_{\text{BH},c} = \left( \frac{a_{12,0}^4 \eta \gamma m_0^{4\gamma}}{7.88 \times 10^{-6}} \right)^{1/(3+4\gamma)}, \quad (9)$$

where  $m_{\text{BH},c}$  and  $m_0$  are the mass of the individual BH at GW dominated coalescence and the initial mass of the BH, both in unit of  $M_{\odot}$ ;  $a_{12,0}$  is the initial separation in unit of  $10^{12}$  cm. The mass evaluated with equation (9) is conservative, because the binary can continue accreting until its merger. However, the correction to  $m_{\text{BH},c}$  will be very small, considering the short duration of the plunging phase. Figure 1 clearly shows how  $a_0$ ,  $m_{\text{BH},0}$ ,  $\tau_{\text{sink}}$  and  $\eta$  determine the final mass  $m_{\text{BH},c}$ :  $a_0$  is the intercept on the vertical axis when the BH has a mass of  $m_{\text{BH},0}$ ; a larger value of  $\tau_{\text{sink}}$  yields a greater power law slope on the declining portion, thus resulting in a smaller  $m_{\text{BH},c}$ ; a larger value of  $\eta$  yields a larger  $m_{\text{BH},c}$ . It is found that the final mass  $m_{\text{BH},c}$  is more sensitive to  $\tau_{\text{sink}}$  than to  $\eta$ .

### 3. DISTRIBUTION OF BH MASS AT COALESCENCE

To determine the population distribution of  $m_{\text{BH},c}$ , the distribution of each parameter on the right side of equation (9) is required. For definiteness, a Gaussian distribution of the initial mass of BHs is assumed, with the mean mass of  $m_{\text{BH},\mu} = 7.8 (M_{\odot})$  and the standard deviation  $m_{\text{BH},\sigma} = 1.2 (M_{\odot})$  (Özel et al. 2010; Farr et al. 2011). The parameter,  $\gamma$ , is calculated from  $\tau_{\text{sink}}$ , the distribution of which is assumed to be uniform between  $\tau_{\text{sink}} = 3$  to  $\tau_{\text{sink}} = 5$ . Finally, the Eddington ratio,  $\eta$ , is assumed to range from 1 to 1000 log-uniformly.

The actual distribution of the orbital separation,  $a$ , of the binary BH system is uncertain. However the Roche radius of the binary BH in orbit about the SMBH should provide an upper limit for  $a$ , for otherwise any binary would be torn apart by the tidal force of the SMBH. The Roche radius  $R_{\text{R}}$  is approximated by:

$$a_{0,\text{max}} = R_{\text{R}} = \left( \frac{2m_{\text{BH}}}{m_{\text{SMBH}}} \right)^{1/3} R_0, \quad (10)$$

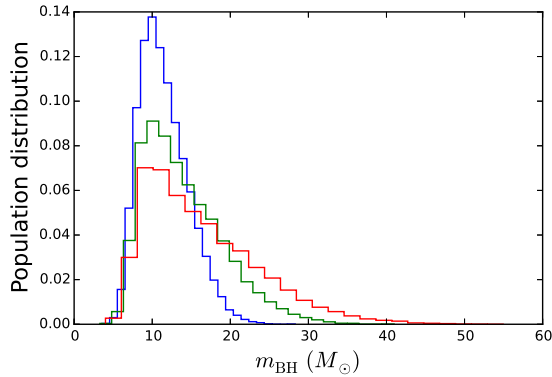


**Figure 2.** The population distribution of  $m_{\text{BH},c}$ . The blue histogram corresponds to the large  $a$  cut-off at  $10^{13}$  cm, the green histogram corresponds to the large  $a$  cut-off at  $10^{14}$  cm and the red histogram corresponds to the cut-off at  $6 \times 10^{14}$  cm.

where  $R_0$  is the initial distance from the binary to the SMBH. If we take the mass of the supermassive BH (in unit of  $M_\odot$ )  $m_{\text{SMBH}} \sim 10^6$ ,  $2m_{\text{BH}} \sim 10$ ,  $R_0 \sim 0.01$  pc, then  $R_{\text{R}} \sim 6 \times 10^{14}$  cm. Stellar interactions with the binary BH can affect the orbital separation distribution and [Bartos et al. \(2017\)](#) considered the ionization of the binary by softening encounters with stars. In this context, the time scale of the ionization can be estimated by:

$$t_{\text{ion}} \approx 10 \times \frac{M_{\text{SMBH}}}{M_{\text{bin}}} t_{\text{orb}}, \quad (11)$$

where  $M_{\text{SMBH}}$  is the mass of the SMBH and  $t_{\text{orb}}$  is the orbital period of the binary around the SMBH. For  $M_{\text{SMBH}} > 10^6 M_\odot$ ,  $M_{\text{bin}} = 20 M_\odot$  and  $R = 0.01$  pc,  $t_{\text{ion}} > 5 \times 10^7$  yr, which is orders of magnitude greater than the merger time scale. Therefore, we can safely ignore this process.

A flat distribution of  $a$  in log space is used, i.e., Öpik's law ([Shatsky & Tokovinin 2002](#); [Lépine & Bongiorno 2007](#); [Kobulnicky & Fryer 2007](#)) with a large  $a$  cut-off as the distribution of  $a$ . There should also be a cut-off at the small  $a$ , where the GW radiation dominates at the outset. This value can be found by setting  $m_{\text{BH},c} = m_0$  in equation (9):

$$a_{12,0,\text{min}} = (7.88 \times 10^{-6} \eta^{-1} \gamma^{-1} m_0^3)^{1/4}. \quad (12)$$

The resulting population distribution of  $M_{\text{BH},c}$  for a range of  $a$  cut-off values is plotted in Fig. 2. The distribution of BH mass peaks at  $\sim 10 M_\odot$ , which is independent of the large  $a$  cut-off, although a larger cut-off extends the tail of the distribution to higher masses. In both distributions, there is a significant fraction of BHs that can increase its mass to greater than  $20 M_\odot$ .

#### 4. MIGRATION TO SMBH

Since the binary is trapped in the accretion disk of an AGN, it will migrate closer to the SMBH due to its interaction. If the orbital separation of the double black hole binary system is much less than the scale height of the disk, the binary can be approximated by a massive point object. We use the disk-satellite interaction to estimate the time scale of migration. Specifically, [Baruteau et al. \(2011\)](#) have shown that if the object is sufficiently massive to open a gap in the disk the horseshoe drag is much reduced and the Lindblad torque balances the viscous torque exerted by the disk (type II migration). The gap-opening criterion is ([Baruteau et al. 2011](#)):

$$\frac{3H}{4R_0} (q/3)^{-1/3} + 50\alpha \left( \frac{H}{R_0} \right)^2 / q < 1. \quad (13)$$

For a SMBH with  $\sim 10^6 M_\odot$ , a binary BH with mass larger than  $20 M_\odot$  (with  $\alpha = 0.01$ ) meets the criterion of type II migration. In this case, the migration time scale is estimated with the equation (6) of [Baruteau et al. \(2011\)](#). We adopt  $m_{\text{SMBH}} = 10^6$ , and use the standard gas pressure dominated disk model ([Shakura & Sunyaev 1973](#))  $H/R_0 \approx 3 \times 10^{-3}$  with Kramer's opacity,  $\alpha = 0.01$  and  $r_0 = 0.01$  pc. This yields  $\tau_{\text{M}} \approx 1.1 \times 10^8$  yrs. Hence, for an Eddington ratio  $\eta > \alpha/10^{-2}$ , the migration time scale does not limit the growth of the BH mass via accretion for low mass AGNs. For AGN with  $m_{\text{SMBH}} > 10^8$ , the migration will be type I and the migration time is  $\sim 10^6$  yr ([Baruteau et al. 2011](#)), which is too short for a significant mass increase of the binary.

## 5. CONCLUSION AND DISCUSSION

The nuclei of galaxies are known to be regions of high stellar density. The star formation rates can be high and the migration of massive objects towards the central region effective. Hence, it is possible that a large population of stellar mass BHs could be harbored in this region, and some of them might be trapped in the gaseous disk around the AGN (Bartos et al. 2017). We show in this Letter that, given a super-Eddington accretion rate ( $\eta$  in range between  $\sim 10$  and 1000), stellar mass binary BHs can accrete significant amount of mass from a circumbinary disk before the GW radiation dominates the coalescence phase with a non-negligible fraction growing to  $> 20 M_\odot$ . The above mentioned evolutionary channel serves as an alternative pathway to produce the unusually massive stellar mass BH binaries detected by LIGO.

### 5.1. The validity of the circular orbit

The binary orbit in a hierarchical triplet may evolve to a large eccentricity due to the Kozai-Lidov mechanism Kozai (1962); Lidov (1962). The first nonzero term of the Kozai-Lidov mechanism is the quadrupole term, which vanishes when the inclination of the inner orbit is smaller than a critical value of  $\sim 39.2^\circ$ . In the next order, i.e., the octupole Kozai-Lidov mechanism, a nearly coplanar inner orbit with very small initial eccentricity will not evolve to a large eccentricity (Lee & Peale 2003; Li et al. 2014). Therefore we limit our discussion to an initially coplanar and circular orbit, which is stable and self-consistent.

### 5.2. Accretion rate onto the binary

Here, we examine the consistency for a super-Eddington accretion rate corresponding to  $\eta = 1 - 1000$ , given the densities in the AGN disk. An upper limit of the accretion rate onto the binary can be estimated with (as in equation (2) of Stone et al. (2017)):

$$\dot{M} = \pi \rho \sigma_{\text{gas}} r_{\text{acc}} \min[r_{\text{acc}}, H], \quad (14)$$

where  $\rho$  and  $H$  are the density and scale height of the AGN disk respectively,  $r_{\text{acc}}$  is the radius of accretion:

$$r_{\text{acc}} = \frac{GM_{\text{bin}}}{\sigma_{\text{gas}}^2}, \quad (15)$$

where  $\sigma^2$  is the squared sum of three terms: 1. the sound speed of the gas  $c_s$ , 2. the velocity shear across the Hill radius of the binary and 3. the relative velocity between the binary and the disk due to eccentric and inclined orbit (see Stone et al. (2017)). In this paper, we consider the binaries in a coplanar and circular orbit around the SMB and, therefore, the third term in  $\sigma_{\text{gas}}^2$  vanishes.  $\rho$  can be estimated with the formula of a standard thin disk:

$$\rho = 5 \times 10^{-11} \left( \frac{\alpha}{0.01} \right)^{-7/10} \eta_{\text{SMBH}}^{11/20} \left( \frac{M_{\text{SMBH}}}{10^6 M_\odot} \right)^{47/40} \left( \frac{R_0}{0.01 \text{ pc}} \right)^{-15/8} \text{ g/cm}^3, \quad (16)$$

where  $\eta_{\text{SMBH}}$  is the Eddington ratio of the SMBH. For  $M_{\text{SMBH}} \sim 10^6 M_\odot$ ,  $R_0 = 0.01 \text{ pc}$ ,  $\alpha = 0.01$  and  $M_{\text{bin}} = 20 M_\odot$ , we find that  $\dot{M}$  is larger than  $10^3$  times of the Eddington rate of the binary as long as  $\eta_{\text{SMBH}} > 0.01$ . When the orbit of the binary is retrograde with respect to the accretion disk of the AGN, the relative velocity between the binary and the gas in the accretion disk dominates  $\sigma_{\text{gas}}^2$ . As a result, the mass inflow rate is much smaller and insufficient to support the required accretion rate. Therefore, we limit our discussion in this paper to the case of a prograde orbit. In the case of super-Eddington accretion, the actual accretion rate onto the BH could be only a fraction of the total matter inflow rate, because substantial mass loss in an outflow is expected (see recent works of Yang et al. (2014) and Jiang et al. (2014) for instance). Hence, the accretion rate in this paper refers to the net value onto the individual BH.  $R_0 = 0.01 \text{ pc}$  is taken as a reference value in the above discussion. For larger radii ( $R_0 > 0.1 \text{ pc}$ ), the AGN disk is no longer stable under its self-gravity and, thus, star formation becomes important (Stone et al. 2017). As a consequence, the physical picture **might need modifications**.

### 5.3. Observational consequences

In our channel, stellar mass BHs can accrete several times their initial mass from the accretion disk. We thus expect that the resulting BHs can become extreme Kerr BHs before coalescence with their spin axes aligned. For such systems, the results of numerical simulations (Healy et al. 2014) indicate that the total energy loss in GW radiation would be

$\sim 10\%$  of the rest mass energy or 2-3 times higher than in the case for a random orientation. Although the currently detected GW events do not provide support for such progenitors, future events may be found which correspond to rapidly spinning and aligned BHs, a likely consequence of our model.

A natural expectation in this formation channel of such GW sources is that they are associated with AGNs. The super-Eddington accretion onto the BHB can give rise to luminous X-ray emission, which may outshine a sub-Eddington accreting AGN in the same wavelength band (see [Bartos et al. 2017](#) and [Stone et al. 2017](#)). Furthermore, after the coalescence of the BHB, remnant matter from the mini disk may fall back onto the newly formed Kerr BH at an even higher rate. Such a possibility may trigger the formation of a relativistic jet through the Blandford-Znajek mechanism ([Blandford & Znajek 1977](#)). As pointed out by [Bartos et al. \(2017\)](#), gamma ray burst-like counterpart could be produced in this case. Besides the radiation at high energies, the jet might also give rise to coherent radio emission, which will be the topic of a future paper.

The authors appreciate the suggestions from reviewers which improved the manuscript a lot. KSC and SXY are supported by a GRF grant under 17310916.

## REFERENCES

- Abbott, B. P., Abbott, R., Abbott, T. D., et al. 2016, *Physical Review X*, 6, 041015
- Abbott, B. P., Abbott, R., Abbott, T. D., et al. 2016, *Physical Review Letters*, 116, 241103
- Abbott, B. P., Abbott, R., Abbott, T. D., et al. 2017, *Physical Review Letters*, 118, 221101
- Abbott, B. P., Abbott, R., Abbott, T. D., et al. 2017, *Physical Review Letters*, 119, 141101
- Aliu, E., Arlen, T., Aune, T., et al. 2011, *ApJL*, 738, L30
- Bartos, I., Kocsis, B., Haiman, Z., & Márka, S. 2017, *ApJ*, 835, 165
- Baruteau, C., Cuadra, J., & Lin, D. N. C. 2011, *ApJ*, 726, 28
- Belczynski, K., Repetto, S., Holz, D. E., et al. 2016, *ApJ*, 819, 108
- Belczynski, K., Holz, D. E., Bulik, T., & O’Shaughnessy, R. 2016, *Nature*, 534, 512
- Blandford, R. D., & Königl, A. 1979, *ApJ*, 232, 34
- Blandford, R. D., & Znajek, R. L. 1977, *MNRAS*, 179, 433
- Bloom, J. S., Giannios, D., Metzger, B. D., et al. 2011, *Science*, 333, 203
- Burrows, D. N., Kennea, J. A., Ghisellini, G., et al. 2011, *Nature*, 476, 421
- Coughlin, E. R., & Begelman, M. C. 2014, *ApJ*, 781, 82
- Dominik, M., Berti, E., O’Shaughnessy, R., et al. 2015, *ApJ*, 806, 263
- Elvis, M., Wilkes, B. J., McDowell, J. C., et al. 1994, *ApJS*, 95, 1
- Farr, W. M., Sravan, N., Cantrell, A., et al. 2011, *ApJ*, 741, 103
- Farris, B. D., Duffell, P., MacFadyen, A. I., & Haiman, Z. 2014, *ApJ*, 783, 134
- Fryer, C. L., & Kalogera, V. 2001, *ApJ*, 554, 548
- Grupe, D., Komossa, S., Leighly, K. M., & Page, K. L. 2010, *ApJS*, 187, 64
- Healy, J., Lousto, C. O., & Zlochower, Y. 2014, *PhRvD*, 90, 104004
- Hirschauer, A. S., Salzer, J. J., Skillman, E. D., et al. 2016, *ApJ*, 822, 108
- Kinugawa, T., Inayoshi, K., Hotokezaka, K., Nakauchi, D., & Nakamura, T. 2014, *MNRAS*, 442, 2963
- Kobulnicky, H. A., & Fryer, C. L. 2007, *ApJ*, 670, 747
- Jiang, Y.-F., Stone, J. M., & Davis, S. W. 2014, *ApJ*, 796, 106
- Kozai, Y. 1962, *AJ*, 67, 591
- Lee, M. H., & Peale, S. J. 2003, *ApJ*, 592, 1201
- Leigh, N. W. C., Geller, A. M., McKernan, B., et al. 2018, *MNRAS*, 474, 5672
- Levin, Y. 2007, *MNRAS*, 374, 515
- Lépine, S., & Bongiorno, B. 2007, *AJ*, 133, 889
- Li, G., Naoz, S., Kocsis, B., & Loeb, A. 2014, *ApJ*, 785, 116
- Lidov, M. L. 1962, *P&SS*, 9, 719
- McKernan, B., Ford, K. E. S., Lyra, W., & Perets, H. B. 2012, *MNRAS*, 425, 460
- McKernan, B., Ford, K. E. S., Kocsis, B., Lyra, W., & Winter, L. M. 2014, *MNRAS*, 441, 900
- Özel, F., Psaltis, D., Narayan, R., & McClintock, J. E. 2010, *ApJ*, 725, 1918
- Shakura, N. I., & Sunyaev, R. A. 1973, *A&A*, 24, 337
- Shatsky, N., & Tokovinin, A. 2002, *A&A*, 382, 92
- Stone, N. C., Metzger, B. D., & Haiman, Z. 2017, *MNRAS*, 464, 946
- Tang, Y., MacFadyen, A., & Haiman, Z. 2017, *MNRAS*, 469, 4258
- Yang, X.-H., Yuan, F., Ohsuga, K., & Bu, D.-F. 2014, *ApJ*, 780, 79